

Do Triatomic Molecules Echo Atomic Periodicity?

Ray Hefferlin, Joshua Barrow

Southern Adventist University

Post Office Box 370, Collegedale, Tennessee 37315, United States

+1-423-236-2869, hefferln@southern.edu

The objective of this work is to test whether vibration frequencies ν_1 of free, ground-state, main-group triatomic molecules manifest a periodicity similar to those of atomic spectroscopic constants. This test and an earlier test on energies of atomization underscore the role of the periodic law as a foundation of chemistry. Using data from four data bases and from computation, we have collected and have mapped ν_1 data in mathematical spaces of fixed-period molecules. These spaces are $8 \times 8 \times 8$ atom cubes with rare-gas molecules on each face. The ν_1 collected from various sources might be of use in searches for cold triatomics in interstellar space.

1. Introduction

Diatomic molecules echo atomic periodicity: plotted data for molecules in series bounded by diatomics having atomic numbers Z_A and Z_B (or both) equal to an atomic magic number are repetitious, and the plots have constant or monotonic amplitude as the molecular masses increase. Gas-phase main-group diatomic molecules AB display this periodic behavior dramatically and allow some reasonably precise predictions to be made [1,2]. The properties that have been studied include internuclear separations r_e [3], vibration frequencies ω_e [3], spring constants k_1 [4], ionization potentials [3], and entire Deslandres tables of band-system Frank-Condon factors[5].

Kong [6] found this same periodicity among contracted internuclear distances of free linear/bent triatomic molecules (Fig. 1). Babaev has shown periodicity in their structural characteristics [7].

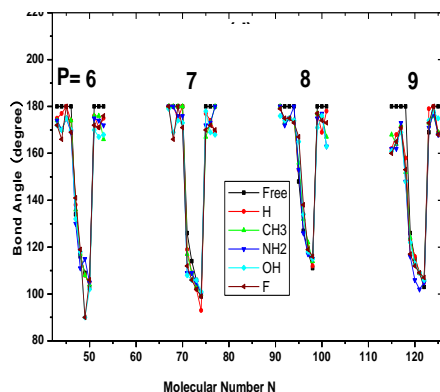


Fig. 1. Percent contracted internuclear distances (dimensionless) [4]. The data are plotted on Kong’s molecular number N , which serves the same role for triatomic molecules in their periodic chart (Fig. 2) as atomic number Z does for atoms in their periodic chart. P is the sum of the three atomic period numbers. The points pertain to free triatomic molecules; the other symbols pertain to “dressed” species, where the atomic number of one outside atom is reduced by 1 and various radicals are attached in its place. When available, the data are from[8]; the remainder are computed at the B3LVP/6/-311G level for $P = 6$ and 7, and at the B3LVP/LanL2DZ level for $P = 8$ and 9.

Kong’s periodic chart of main-group triatomic molecules (Fig. 2) has the sum of the group numbers (3 to 24) horizontally, and the sum of the period numbers vertically. A molecule whose atoms are in Mendeleev-chart periods 2,2, 4 has a period sum $P = 8$. The first two rows of Kong’s chart contain species of no interest in this research. Triatomic molecular numbers, above and to the left of the molecular name, are assigned from left to right in $P = 6$, then in $P = 7$, etc.

$P \backslash G$	1	2	3	4	5	6	7	8	9	10	11	12	13	14	15	16	17	18	19	20	21	22	23	24	
4	¹ LiH ₂ ⁺	² LiH ₂ ⁺	³ LiH ₂	⁴ BeH ₂	⁵ BH ₂	⁶ CH ₂	⁷ NH ₂	⁸ H ₂ O	⁹ H ₂ F	¹⁰ H ₂ Ne	¹¹ HHeNe	¹² He ₂ Ne													
5	¹³ LiHe ₂	¹⁴ Li ₂ He	¹⁵ Li ₂ H	¹⁶ HLiHe	¹⁷ HBe ₂	¹⁸ HBeB	¹⁹ B ₂ H	²⁰ HBC	²¹ C ₂ H	²² H ₂ CN	²³ N ₂ H	²⁴ HNO	²⁵ HO ₂	²⁶ HOF	²⁷ HF ₂	²⁸ HFNe	²⁹ HNNe ₂	³⁰ HeNe ₂							
6	³¹ LiAr ₂	³² Li ₂ Ne	³³ Li ₃	³⁴ Li ₂ Be	³⁵ LiBe ₂	³⁶ Be ₃	³⁷ Be ₂ B	³⁸ BeB ₂	³⁹ B ₃	⁴⁰ B ₂ C	⁴¹ C ₂ B	⁴² C ₃	⁴³ C ₂ N	⁴⁴ CN ₂	⁴⁵ N ₃	⁴⁶ N ₂ O	⁴⁷ NO ₂	⁴⁸ O ₃	⁴⁹ FO ₂	⁵⁰ F ₂ O	⁵¹ F ₃	⁵² NeF ₂	⁵³ Ne ₂ F	⁵⁴ Ne ₃	
7	⁵⁵ NaNe ₂	⁵⁶ Li ₂ Ar	⁵⁷ Li ₂ Na	⁵⁸ Li ₂ Mg	⁵⁹ NaBe ₂	⁶⁰ Be ₂ Mg	⁶¹ NaBe ₂	⁶² Be ₂ Mg	⁶³ Be ₂ Al	⁶⁴ B ₂ Si	⁶⁵ AlC ₂	⁶⁶ SiC ₂	⁶⁷ C ₂ P	⁶⁸ SiN ₂	⁶⁹ N ₂ P	⁷⁰ N ₂ S	⁷¹ PO ₂	⁷² SO ₂	⁷³ ClO ₂	⁷⁴ SF ₂	⁷⁵ ClF ₂	⁷⁶ ArF ₂	⁷⁷ Ne ₂ Cl	⁷⁸ Ne ₂ Ar	
8	⁷⁹ LiAr ₂	⁸⁰ Na ₂ Ne	⁸¹ Na ₂ Li	⁸² Na ₂ Be	⁸³ LiMg ₂	⁸⁴ Mg ₂ Be	⁸⁵ Mg ₂ B	⁸⁶ BeAl ₂	⁸⁷ Al ₂ B	⁸⁸ Al ₂ C	⁸⁹ Si ₂ B	⁹⁰ Si ₂ C	⁹¹ Si ₂ N	⁹² CP ₂	⁹³ P ₂ N	⁹⁴ P ₂ O	⁹⁵ NS ₂	⁹⁶ S ₂ O	⁹⁷ S ₂ F	⁹⁸ Cl ₂ O	⁹⁹ Cl ₂ F	¹⁰⁰ NeCl ₂	¹⁰¹ Ar ₂ F	¹⁰² Ar ₂ Ne	
9	¹⁰³ NaAr ₂	¹⁰⁴ Na ₂ Ar	¹⁰⁵ Na ₃	¹⁰⁶ Na ₂ Mg	¹⁰⁷ NaMg ₂	¹⁰⁸ Mg ₃	¹⁰⁹ Mg ₂ Al	¹¹⁰ MgAl ₂	¹¹¹ Al ₃	¹¹² Al ₂ Si	¹¹³ AlSi ₂	¹¹⁴ Si ₃	¹¹⁵ Si ₂ P	¹¹⁶ SiP ₂	¹¹⁷ P ₃	¹¹⁸ P ₂ S	¹¹⁹ PS ₂	¹²⁰ S ₃	¹²¹ S ₂ Cl	¹²² S ₂ Cl ₂	¹²³ Cl ₃	¹²⁴ ArCl ₂	¹²⁵ Ar ₂ Cl	¹²⁶ Ar ₃	
10	¹²⁷ KAr ₂	¹²⁸ Na ₂ Kr	¹²⁹ Na ₂ K	¹³⁰ Na ₂ Ca	¹³¹ KMg ₂	¹³² Mg ₂ Ca	¹³³ Mg ₂ Ga	¹³⁴ CaAl ₂	¹³⁵ Al ₂ Ga	¹³⁶ Al ₂ Ge	¹³⁷ GaSi ₂	¹³⁸ Si ₂ Ge	¹³⁹ Si ₂ As	¹⁴⁰ GeP ₂	¹⁴¹ P ₂ As	¹⁴² P ₂ Se	¹⁴³ As ₂ S ₂	¹⁴⁴ SeS ₂	¹⁴⁵ S ₂ Br ₂	¹⁴⁶ Se ₂ Cl	¹⁴⁷ BrCl ₂	¹⁴⁸ KrCl ₂	¹⁴⁹ Ar ₂ Br	¹⁵⁰ Ar ₂ Kr	
11	¹⁵¹ NaKr ₂	¹⁵² K ₂ Ar	¹⁵³ NaK ₂	¹⁵⁴ K ₂ Mg	¹⁵⁵ NaCa ₂	¹⁵⁶ MgCa ₂	¹⁵⁷ Ca ₂ Al	¹⁵⁸ MgGa ₂	¹⁵⁹ AlGa ₂	¹⁶⁰ Ga ₂ Si	¹⁶¹ AlGe ₂	¹⁶² SiGe ₂	¹⁶³ Ge ₂ P	¹⁶⁴ SiAs ₂	¹⁶⁵ PAs ₂	¹⁶⁶ As ₂ S	¹⁶⁷ Se ₂ P	¹⁶⁸ Se ₂ S	¹⁶⁹ SeCl ₂	¹⁷⁰ S ₂ Br ₂	¹⁷¹ Br ₂ Cl	¹⁷² ArBr ₂	¹⁷³ Kr ₂ Cl	¹⁷⁴ ArKr ₂	
12	¹⁷⁵ KKr ₂	¹⁷⁶ K ₂ Ar	¹⁷⁷ K ₃	¹⁷⁸ K ₂ Ca	¹⁷⁹ Ca ₂ K	¹⁸⁰ Ca ₃	¹⁸¹ Ca ₂ Ga	¹⁸² CaGa ₂	¹⁸³ Ga ₃	¹⁸⁴ Ga ₂ Ge	¹⁸⁵ GaGe ₂	¹⁸⁶ Ge ₃	¹⁸⁷ Ge ₂ As	¹⁸⁸ GeAs ₂	¹⁸⁹ As ₃	¹⁹⁰ As ₂ Se	¹⁹¹ AsSe ₂	¹⁹² Se ₃	¹⁹³ Se ₂ Br	¹⁹⁴ SeBr ₂	¹⁹⁵ Br ₃	¹⁹⁶ KrBr ₂	¹⁹⁷ Kr ₂ Br	¹⁹⁸ Kr ₃	
13	¹⁹⁹ RbKr ₂	²⁰⁰ K ₂ Xe	²⁰¹ K ₂ Rb	²⁰² K ₂ Sr	²⁰³ RbCa ₂	²⁰⁴ Ca ₂ Sr	²⁰⁵ Ca ₂ In	²⁰⁶ SrGa ₂	²⁰⁷ Ga ₂ In	²⁰⁸ Ga ₂ Sn	²⁰⁹ InGe ₂	²¹⁰ Se ₂ Sn	²¹¹ Ge ₂ Sb	²¹² SnAs ₂	²¹³ As ₂ Sb	²¹⁴ As ₂ Te	²¹⁵ SbSe ₂	²¹⁶ Se ₂ Te	²¹⁷ Se ₂ I	²¹⁸ TeBr ₂	²¹⁹ Br ₂ Cl	²²⁰ XeBr ₂	²²¹ Kr ₂ I	²²² Kr ₂ Xe	
14	²³³ KXe ₂	²³⁴ Rb ₂ Kr	²³⁵ KRb ₂	²³⁶ Rb ₂ Ca	²³⁷ KSr ₂	²³⁸ CaSr ₂	²³⁹ Sr ₂ Ga	²⁴⁰ CaIn ₂	²⁴¹ GaIn ₂	²⁴² In ₂ Ge	²⁴³ GaSn ₂	²⁴⁴ SeSn ₂	²⁴⁵ SnAs ₂	²⁴⁶ GeSb ₂	²⁴⁷ AsSb ₂	²⁴⁸ Sb ₂ Se	²⁴⁹ AsTe ₂	²⁵⁰ SeTe ₂	²⁵¹ Te ₂ Br	²⁵² SeI ₂	²⁵³ BrI ₂	²⁵⁴ KrI ₂	²⁵⁵ Xe ₂ Br	²⁵⁶ KrXe ₂	
15	²⁵⁷ RbXe ₂	²⁵⁸ Rb ₂ Xe	²⁵⁹ Rb ₃	²⁶⁰ Rb ₂ Sr	²⁶¹ RbSr ₂	²⁶² Sr ₃	²⁶³ Sr ₂ In	²⁶⁴ SrIn ₂	²⁶⁵ In ₃	²⁶⁶ SnIn ₂	²⁶⁷ Sn ₂ In	²⁶⁸ Sn ₃	²⁶⁹ SnSb ₂	²⁷⁰ Sn ₂ Sb	²⁷¹ Sb ₃	²⁷² Sb ₂ Te	²⁷³ SbTe ₂	²⁷⁴ Te ₃	²⁷⁵ Te ₂ I	²⁷⁶ TeI ₂	²⁷⁷ I ₃	²⁷⁸ XeI ₂	²⁷⁹ Xe ₂ I	²⁸⁰ Xe ₃	

Fig. 2. Kong's periodic system of main-group triatomic molecules [9]. The table has the sums of the atomic group and period numbers G from left to right and P down from top to bottom. Rows $P = 4$ and 5 are devoted to hydrides and alkali metal rare gas molecules. The cells show only the simplest triatomic molecules; the other isoelectronic species in cells can be found by proton shifting.

These and other results for diatomic and triatomic molecules underscore the role of the *periodic law* as a foundation of chemistry, and thus support the argument that chemistry is not a special case of physics (the subject of prolonged debate [*e.g.* 10]).

The objectives of this work are to test for periodicity in heats of atomization of free triatomic molecules, and in addition to prepare for testing triatomic molecular longitudinal symmetric-stretch vibration frequencies ν_1 . The test for this property will entail additional work; the beginning of this work – entailing only $P = 6$ molecules – occupies much of this paper. The spectroscopic constant ν_1 was chosen partly with the hope that it may be distributed in triatomic molecular space as smoothly as diatomic molecular vibration frequencies are in diatomic molecular space [11]. It was also chosen in the hope that the collected data might assist astrophysicists in searches for cold triatomic molecules in circumstellar space.

2. Theory

2.1. Chemical considerations

This investigation does not address the whether any particular free triatomic exists in the observable universe or in experimental apparatus. All of them are considered candidates for existence in some unexplored location in the cosmos or for a brief existence as transition species.

Aside from this, considerations such as bond types, bond orders, cyclic isomers, multiplicities, and behavior when in the solid or liquid state, are ignored in this study.

2.2. Molecular mechanics

The symmetric-stretch vibration frequency of a linear, symmetric, triatomic molecule is given by the standard equation for a mass hanging on a spring:

$$\nu_1 = (1/2\pi)\sqrt{k_1/m} \quad , \quad (1)$$

where k_1 is the force constant appropriate for the motion and m is the mass of either outer atom [12]. The equation for ν_1 is almost the same as that for the vibration frequency ω_e of a diatomic molecule; the only change needed in Eq. (1) is to replace m by the reduced mass:

$$\omega_e = (1/2\pi)\sqrt{k_1/\mu} \quad . \quad (2)$$

It follows that ν_1 of a linear, symmetric, triatomic molecule ABA can be obtained from ω_e of the diatomic molecule AB by

$$\nu_1 = \omega_e\sqrt{\mu/m} \quad . \quad (3)$$

This conversion will be used in the section on data acquisition. The equations for non-linear, non-symmetric, or non-linear and non-symmetric triatomics [12] were not used in this work.

2.3. The space for linear/bent triatomic molecules

Being able to visualize this mathematical space is essential for understanding what follows in this paper. First, imagine an $8 \times 8 \times 8$ -atom cube populated by main-group period-2 atoms with rare-gas molecules on three faces. Then generalize to many such cubes, ranging from $(R_1, R_2, R_3) = (2, 2, 2)$ to $(7, 7, 7)$ (Fig. 3) where R_i is the period number of atom i . The result is the molecular mathematical space for neutral main-group triatomic molecules.

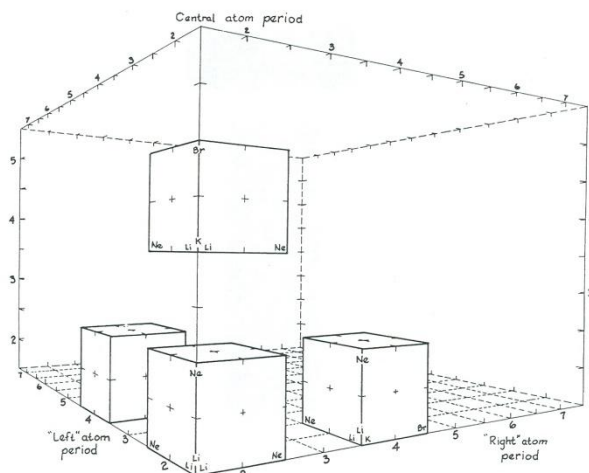


Fig. 3. The space for main-group triatomic molecules formed from atoms $(R_1, R_2, R_3) = (2, 2, 2)$ to $(7, 5, 7)$; hydrogen and helium ($R_i = 1$) are omitted. The diagram is symmetric with respect to reflection in a plane containing the closest and the farthest edges of the space; hence the cube with periods $(R_1, R_2, R_3) = (4, 2, 2)$ contains the same molecules as does the cube $(2, 2, 4)$.

The features inside the individual cubes (subspaces) are important. Fig. 4 shows horizontal cuts made for various central atoms; they are enumerated by the group number, C_2 , of the central atom. If the cube is selected from $R_1 = R_2$, then the molecules on each cut are symmetric to reflection through the line $C_1 = C_3$; otherwise species on opposite sides of the plane $C_1 = C_3$ are not redundant.

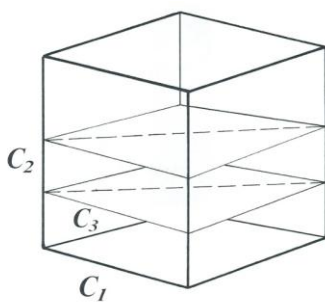


Fig. 4. Sample horizontal cuts for different central atoms, C_2 , of any cube in Fig. 3. The figure is rotated approximately 90° with respect to those in Fig. 3 and is not to scale.

The cubes may be sliced by other planes, for example planes containing isoelectronic molecules (Fig. 5). The slicing may be done while the cubes are all packed into the space of Fig. 1, with the result that an isoelectronic sequence will have members in more than one cube.

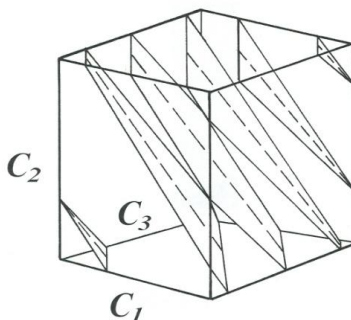


Fig. 5. Sample isoelectronic slices in any subspace of Fig. 3. As the total electron count n_e increases, the slices progress from a triangle at the lower left, to a truncated triangle, to a hexagon, and back with reverse orientation toward the upper right. The dashed lines in the figure pass through the locations of symmetric molecules that lie on the vertical plane $C_1 = C_3$ of Fig. 3.

3. Data acquisition

3.1. Tabulated triatomic vibration frequencies

The National Institute of Science and Technology Webbook[8] provides data for many known triatomics. Webbook data were used except for those ABC species where ν_1 and ν_3 were identified as the “AB stretch” and “BC stretch.” The most recent ν_1 datum was always used, without regard to the method used to obtain it. An earlier compilation by Krasnov[13] was also consulted to obtain vibration frequencies. Its values were used where the Webbook was silent.

3.2. Linear symmetric molecules as a special case

The “Handbook for Physics and Chemistry” [14] and “Constants of Diatomic Molecules” by Huber and Herzberg [15], provide ω_e for two-atom (AB) molecules. Using Eq. (3) and a table of atomic masses make it possible to calculate ν_1 for the triatomics ABA. This calculation is very useful because data for several triatomic molecules can be obtained that are not accessible in [8] or [13]. Table 1 presents data obtained in this way.

Table 1. Linear symmetric triatomic symmetric-stretch vibration frequencies obtained using Eq. (3). All values have been rounded to one significant figure after the decimal point.

(R_1, R_2, R_3)	n_e	Molecule		ν_1	Reference for ω_e
		Diatomic	Triatomic		
(2,2,2)	13	LiN	LiNLi	379.5	[15]
	14	LiO	LiOLi	470.1	[15]
	15	LiF	LiFLi	472.8	[15]
	15	B ₂	B ₃	750.2	[15]
	22	BeF ^a	FBeF	707.5	[15]
	22	NO	ONO	1301.0	[15]
	22	NO	NON	1390.3	[15]
	24	BF	FBF	849.3	[15]

^a The datum “corresponds to $\Delta G(1/2)$ or the lowest observed integral”

3.3. Computations for Molecules

We employed two *ab initio* chemistry modeling programs with the WebMo graphical user interface. Within the graphical user interface, a molecule was built each time with single bonds connecting the atoms. The molecule then had its mechanics “optimized” for bond lengths and bond angle. The Hartree-Fock method, the “optimization and vibration Frequency” option, the “unrestricted” reference, and the automatically recommended multiplicity were always used; then the computer determined the optimum bond lengths and angles for the molecule.

This protocol was used for each of the several basis sets. We primarily used 6-31+G(d) and 6-311+G(d,p) (identical to 6-31+G* and 6-311+G** respectively) basis sets using the QChem software. We also used aug-cc-pVDZ and pVQZ basis sets with PSI4 software. These latter choices took substantially more computational time than any QChem bases: while either basis in QChem would take between 1 and 20 minutes, and aug-cc-pVDZ within PSI4 would take just under an hour’s time, aug-cc-pVQZ could run for as many as 30 hours per molecule.

While queuing jobs for the computer to process throughout the day and overnight, we would request it to run using three bases for each molecule: usually 6-311+G**, aug-cc-pVDZ, and aug-cc-pVQZ. By doing so, we hoped to obtain at least one successful result; to save time; and to establish whether or not the computer agreed with itself for a given molecule.

The symbols ν_1 , ν_2 , and ν_3 are almost always used to represent the symmetric-stretch, bending, and asymmetric-stretch vibration modes. Occasionally the values found were such that ν_1 , ν_2 , and ν_3 are in actuality ν_3 , ν_2 , and ν_1 ; for these few ν_1 and ν_3 were reversed.

4. Analysis of data

4.1. Specifics of the molecular space

As data, they were placed in bins of constant total electron count n_e . It is here that Fig. 5 must be consulted – in particular, the dashed lines within the various planes of fixed n_e . Falling along these dashed lines are symmetric molecules enumerated by C_2 . Now consider the subspace containing molecules with atoms from $(R_1, R_2, R_3) = (2, 2, 2)$. Species containing rare-gas atoms were ignored, so the least and greatest total electron counts pertain to Li_3 and F_3 :

$$C_1 + C_2 + C_3 = k, \quad 3 \leq k \leq 21 \quad . \quad (4)$$

where C_i is the integer group number of atom i in short form periodic charts, $1 \leq C_i \leq 7$, and k is a constant. Within each bin, the data were entered in order of C_2 . If the molecules are symmetric, $C_1 = C_3$, and

$$C_1 = (k - C_2)/2 \quad . \quad (5)$$

Table 2 shows solutions of this equation for integer values of C_2 and C_1 that yield symmetric molecules bounded, in C_2 for a given k , by species with rare-gas atoms. Several aspects deserve attention:

- The bins do not have the same numbers of occupants
- The generalization to non-symmetric molecules is trivial: decrease C_1 by 1 and increase C_3 by 1. This process generates new molecules which could be horizontal in Table 1 and which would eventually end with rare-gas molecules.
- The generalization to molecules with atoms from other periods is trivial

Table 2. Solutions of Eq. (5) for $(R_1, R_2, R_3) = (2, 2, 2)$ molecules. Values of C_1 , C_2 , or n_e that are half-integer or negative, and molecules with one or more rare-gas atom, have been deleted.

k	C_2	C_1	n_e	Molecule	k	C_2	C_1	n_e	Molecule
4	2	1	10	LiBeLi	18	12	2	5	BBeB
5	1	2	11	BeLiBe	12	4	4	4	CCC
5	3	1		LiBLi	12	6	3	3	BOB
6	2	2	12	BeBeBe	19	13	1	6	OLiO
6	4	1		LiCLi	13	3	5	5	NBN
7	1	3	13	BLiB	13	5	4	4	CNC
7	3	2		BeBBe	13	7	3	3	BFB
7	5	1		LiNLi	20	14	2	6	OBeO
8	2	3	14	BBeB	14	4	4	5	NCN
8	4	2		BeCBe	14	6	4	4	COC
8	6	1		LiOLi	21	15	1	7	FLiF
9	1	4		CLiC	15	3	6	6	OBO
9	3	3	15	BBB	15	5	5	5	NNN
9	5	2		BeNBe	15	7	4	4	CFC
9	7	1		LiFLi	22	16	2	7	FBeB
10	2	4	16	CBeC	16	4	6	6	OCO
10	4	3		BCB	16	6	5	5	NON
10	6	2		BeOBe	23	17	3	7	FBF
11	1	5	17	NLiN	17	5	6	6	ONO
11	3	4		CBC	17	7	5	5	NFN
11	5	3		BNB	24	18	4	7	FCF
11	7	2		BeFBe	18	6	6	6	OOO
Continued at right					25	19	5	7	FNF
					26	20	6	7	FOF

4.2. Tabulating the results

As the molecular vibration frequencies were being placed into a master file, they were plotted on C_2 (Fig. 6) as a running check on the data-entry process. In the cases where two or more tabulated or computational results for a given molecules did not fall as close or closer together than shown in the figure, then the outliers were dropped.

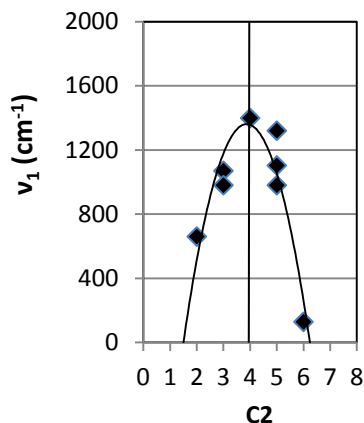


Fig. 6. A graphic produced as a cross-check while data were being introduced into the portion of the main file for molecules with $n_e = 21$. Vibration frequencies ν_1 are plotted on C_2 . $C_2 = 0$ and 8 relate to rare-gas molecules. The parabolic fit has only a suggestive role; a more realistic curve might intersect the abscissa at 1 and 7. The very low-value datum at $C_2 = 6$ would normally have been ignored but in this case was retained. The figure gives a sense of the spreads of data for which averages and error measures were calculated. Additional discussion of these measures follows in Section 4.3.

The resulting data are presented in Table 3. The molecules shown are far from being the totality of all molecules that would fill their space for several reasons:

- Large numbers of molecules are not in the tables and requests for computational values failed
- Any molecular computation which resulted in imaginary or negative values of ν_1 , or presented the molecule as being cyclic, were discarded
- Any result for ν_1 and ν_3 designated as AB and BC stretches was discarded
- Results including single- or double-digit vibration frequencies were dropped except if the molecules' C_2 values were close to the limiting values (Section 4.2)
- If data from **K**, **H**, or **P** differed seriously from **W** (bold-face symbols defined in Table 3) or from the surrounding ν_1 in Fig. 6, they were ignored

Table 3. Data for molecules from (R1,R2,R3) = (2,2,2) in order of n_e and then C_2 . The averages are derived from *computed* values (**A**, aug-cc-pVDZ; **C**, aug-cc-pVQZ; **D**, 6-311+G**); **L**, 6-31G(d); and **M**, 6-311+G(d,p)); and from *tabulated* values (**W** [8] and **K** [13]); and from **P** [14] and **H** [15] with Eq. (3)). “**2M;KW**” means the **M** was successful two times and slightly different tabulated values were found in **K** and **W**. If two sources contributed, then the half-difference error is shown in column 4; if more contributed then the sample standard deviation is shown. All values are rounded to one significant figure after the decimal. End-notes to the table state the causes of percent errors in excess of 10%.

n_e	Species	Mean ν_1 (cm ⁻¹)	½ diff. error, or σ	Percent of mean	Table or basis
11	LiBeBe	388.4			C
12	BeBeBe	539.5	1.5	0.3	AD
	LiBeB	356.6	40.0	11.2 ^a	AD
	LiBBe	533.2	0.2	0.0	2C
	LiCLi	570.9			A
13	BBeBe	443.8			M
	LiCBe	626.3			M
	LiNLi	772.8			A
14	BBeB	762.2			A
	BeBB	635.4			A
	LiOLi	817.2	33.2	3.8	A,C;W
15	BBeC	534.6			A
	BBB	535.3			H
	BeCB	1218.6	0.3	0.0	C,D
	BeNBe	1290.3	2.0	0.2	2D
	BNLi	764.1	2.8	0.4	AD
	BeOLi	840.1			C
	LiFLi	672.2			H
16	BeBeO	693.2			W
	CBeC	1130.0	1.3	0.1	CD
	LiNC	2080.4			K
	BeOBe	1083.4	38.4	3.5	2M;KW
17	BBeO	475.4 ^b			L
	CBeN	760.8			A
	BeBeF	458.4	179.4	39.1 ^a	CD
	BeBO	646.9	31.7	4.9	D,M
	LiBF	243.3	21.9	9.0	AC3G
	CCB	1526.1			M
	BNB	1290.8			L

17	LiCO BeOB	652.2 493.3			M M
18	NBeN BBO CCC BCN BOB BeFB LiFC	520.0 617.5 1224.5 863.7 1113.0 19.4 605.0	48.7 177.0	7.9 20.5 ^c	A C,M W ACDM M M M
19	OLiO CNC BNN BeNO LiOF BeON BOC	719.7 1123.0 957.4 759.6 804.1 1439.5 1141.5	77.0 0.7 154.2	6.9 0.1 20.3 ^d	W MK M;K M,W M M M
20	OBeO NCN CCO COC	1060.5 1338.0 1970.9 1096.1	122.1	9.1	M 2A;W W M
21	OBeF OBO NBF NCO BNF CNO NNN BeOF	660.1 1070.0 980.4 1398.7 980.3 1103.2 1320.0 128.6			A W A A M A W 2A
22	FBeF OBF OCO NCF BOF NON	735.6 1076.1 1425.7 1205.0 1059.8 1076.8	31.1 ^e 37.0 92.7	2.6 3.4 6.5	A;H,W A,C,D;W D;W C A A
23	FBF OCF ONO FCF	1153.0 1861.6 1318.0 1225.1			W W W W
24	FNO NOF OOO FNF	945.4 1103.0 1103.0 1075.0	0.6	0.1	D,M W W W
25	OOF	1491.0	4.0	0.3	K,W

- ^a The computation from 6-311+G** is considerably higher in this instance than that for aug-c-pVDZ
- ^b This 6-31G(d) value is next to a rare gas vibration frequency, presumed to be very small. If the 6-311+G(d,p) result of 1053.8 is retained, then columns 2 to 4 contain 746.6, 289.2, and 37.8,
- ^c The computation from 6-311+G** is again considerably higher than those for aug-c-pVDZ and pVQZ, and 6-311+G(d,p)
- ^d The result from 6-311+G(d,p) is low with respect to the Webbook value.
- ^e The Huber and Herzberg value used in Eq. (4) is doubtful because it may refer to ω_e for a vibrational level higher than $v'' = 0$.

4.3. The distribution of molecules in their space

For every molecule ABC the data in the file were reversed so as to include the molecule CBA. All of these were then plotted in the (C_1, C_2, C_3) coordinates of $(R_1, R_2, R_3) = (2, 2, 2)$. Fig. 7 shows ν_1 having the highest values, from 2230 down to 1200 cm^{-1} . It can be seen that they all have carbon, nitrogen, and oxygen as their central atoms. Fig. 8 presents all of the ν_1 values gleaned in this study.

As explained in Section 4.2, the failure of Fig. 8 to show a completely filled molecular sub-space is due to the absence of so many molecules in the tables and to the failure of many of the computations.

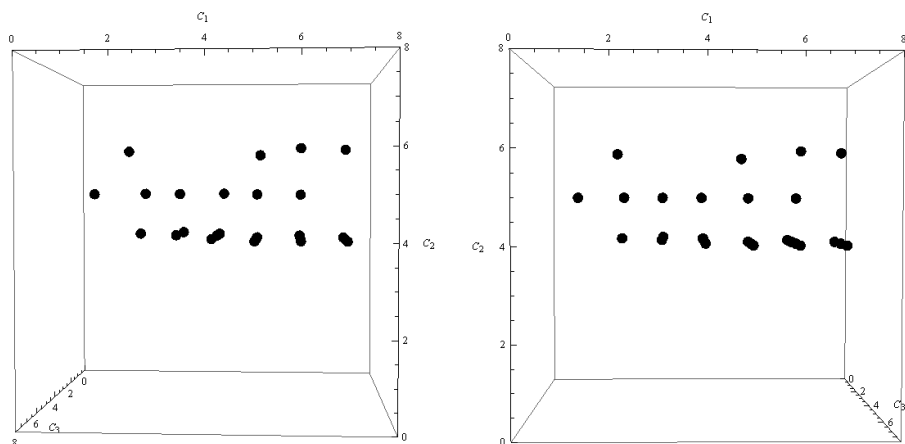


Fig. 7. Stereoscopic view of vibration frequencies for molecules in the subspace $(R_1, R_2, R_3) = (2, 2, 2)$ having the high-end ν_1 values from 2230 down to 1200 cm^{-1} . The data are symmetric with respect to reflection through the $C_1 = C_3$ plane, which passes through the near vertical edge at right and the far vertical edge at left.

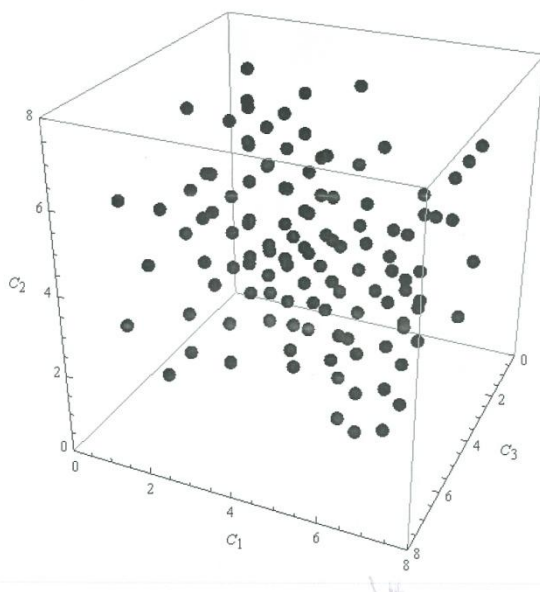


Fig. 8. Vibration frequencies for all molecules in the subspace $(R_1, R_2, R_3) = (2, 2, 2)$. This subspace is the cube in Fig. (3) that lies at the bottom and close to the reader..

4.4. Analysis of errors

After the entries were vetted as discussed above Fig. 6, and before the introduction of reversed values (Section 4.3), the data for each molecule having more than one entry were averaged.

Percent errors of these means were estimated as follows: if there are two data, $v_{1,1}$ and $v_{1,2}$, (29% of the instances), then

$$\text{Percent error} = ((v_{1,1} - v_{1,2})/2) * 100/X \quad , \quad (6)$$

where X is the mean of the two data. If there are more than two data (12% of the instances) the percent error of each datum is

$$\text{Percent error} = \sigma(v_1) * 100/X \quad , \quad (7)$$

Where X is the mean of all the data.

The percent errors of means of computed vibration frequencies are shown in Table 4.

Table 4. Mean combined random and systematic errors (rows 1 to 5, where X is the NIST Webbook), and mean random errors (rows 6 to 10, where X represents the average for results from all the computations or compilations). Basis sets not shown had no result or one obtained result. All values are rounded to one significant figure after the decimal point.

Table or basis set	X	Entries	Mean v_1 error in cm^{-1}	Percent error of mean
aug-cc-pVDZ	[8]	2	9.3	9.6
aug-cc-pVQZ	[8]	8	-5.5	18.4
6-311+G**	[8]	5	-12.2	27.5
6-311+G(d,p)	[8]	4 ^a	5.9	3.7
[13]	[8]	3	-1.1	3.2
aug-cc-pVDZ	Our mean	25	-1.5	7.0
aug-cc-pVQZ	Our mean	21	-2.8	12.4
6-311+G**	Our mean	28	0.9	5.3
6-311+G(d,p)	Our mean	7	1.6	4.4
[14]	Our mean	3	0.0	2.6

^a One two-digit value of v_1 was omitted from the statistics. This value was adjacent to a rare-gas molecule and contributed to the correct decline of the parabola (Fig. 6) toward zero.

In one case (row 4) the standard deviation is smaller than the average. In the other cases, the averages are *statistically* not different from zero.

5. Demonstration of periodicity

Up to this point there has been only one test of periodicity (Fig. 1). It is time to consider another test. Triatomic molecular energies of atomization provide an excellent manifestation of periodicity. The test, however, requires thought concerning independent variables, for it is difficult to visualize trends in the six-dimensional space, $R_1, C_1, R_2, C_2, R_3,$ and C_3 , within which the data for triatomic molecules lie. Therefore, a collapsed coordinate system is used. The coordinates of this system are $n_e, C_2,$ and (from frame to frame below) $f(R)$, which is

$$f(R) = R_1R_2 + R_2R_3 \quad . \quad (9)$$

This formula for $f(R)$ was found earlier [16] by plotting data for fixed-group molecules on various functions of the atomic period numbers, such as $R_1 + R_2 + R_3$ and $R_1R_2R_3$. From among these, the plots showed $f(R)$ to be a marginally superior independent variable for most properties.

It is remarkable that data for spectroscopic constants of fixed-period [fixed $f(R)$] molecules are often found to have similar values in series with fixed

$$G(C) = C_1+2C_2+C_3 = (C_1+C_2) + (C_2+C_3), \quad (9)$$

as often, or even more so, than in isoelectronic series (with fixed $C_1+C_2+C_3$). Eqs. (8) and (9) define a simple Diatomics-in-Molecules method for data plotting.

Energies of atomization for molecules with fixed period numbers $f(R) = R_1R_2 + R_2R_3$, plotted on coordinates enumerated by n_e and C_2 are shown in the following figures, which clearly show periodicity of triatomic $\Delta_a H$.

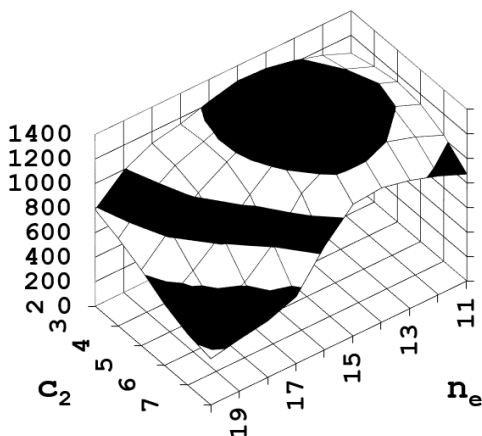


Fig. 9. $\Delta_a H$ in kJ/mol for $f(R) = 8$, *i.e.*, $(R_1, R_2, R_3) = (2, 2, 2)$. This plot and those that follow are the result of a neural-network model built from available data.

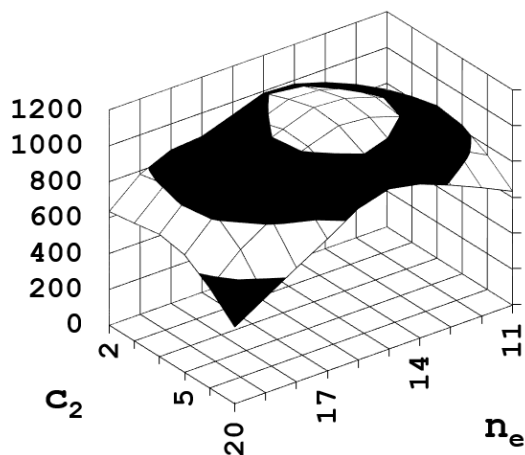


Fig. 10. $\Delta_a H$ in kJ/mol for $f(R) = 16$, *i.e.*, $(R_1, R_2, R_3) = (2, 4, 2)$, $(4, 2, 4)$, $(6, 2, 2)$, and $(2, 2, 6)$. Permuted period numbers do not result in redundancies, but for each $f(R)$ any intersection of the fishnet surface may represent several molecules. Hence, given both $f(R)$ it follows that each intersection may be populated by very many molecules. The ordinates of the graph are neural-network “averages” based on all known data, so it is clear that any attempt to predict $\Delta_a H$ at any location would be futile.

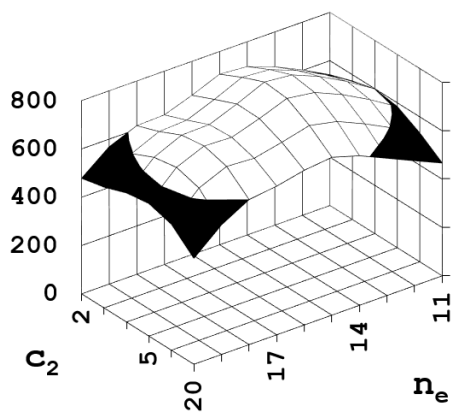


Fig. 11. Same as Fig. 10 except for $f(R) = 28$, *i.e.*, $(R_1, R_2, R_3) = (5, 2, 4)$, $(4, 2, 5)$, $(5, 6, 2)$, $(6, 2, 5)$, $(2, 7, 2)$, and $(7, 2, 7)$. A second hump at $n_e = 17$ is visible.

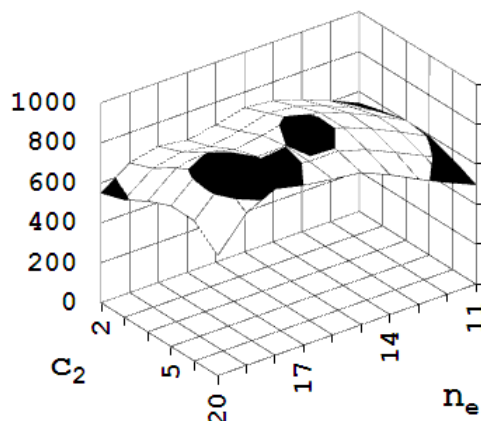


Fig. 12. Same as Fig. 10 except for $f(R) = (5,6,5)$ or $(6,5,6) = 60$. The amplitudes of the figures decrease monotonically as $f(R)$ increases, a requisite for claiming periodic behavior. The second hump visible in Fig. 11 has grown relatively larger while still within the monotonic constraint. .

6. Discussion

Periodicity among triatomic molecules has been demonstrated in their bond angles (Fig. 1) and heats of atomization (Figs. 9-12). Data accumulated, but not included in this report, hint strongly at periodicity among the bond lengths.

The ν_1 values in Table 3, some from [8] or [13] and some determined in this work, could be of use in a search for free triatomic molecules in interstellar space. There exists a NIST data base containing high-precision long-wavelength spectral features, but for a limited number of triatomic molecules [17].

7. Acknowledgements

The School of Chemistry and Biochemistry of the Georgia Institute of Technology has our profound thanks for allowing access to QChem and to the open-source *ab initio* electronic structure computer program PSI4[18]. We thank Jonathan King for his participation in the computation process. We also thank Nels Angelin (of Nels Angelin Drafting, Apison, Tennessee), Dr. Blake Laing and Dr. Ken Caviness (of Southern Adventist University) for contributing to the graphics in this article.

References

- [1] Hefferlin, R. Vibration frequencies using least squares and neural networks for 50 new *s* and *p* electron diatomics, *J. Quant. Spectr. Rad. Transfer*, 111, 71-77 (2010).
- [2] Hefferlin, R. Internuclear separations using least squares and neural networks for 46 new main-group diatomics. *Int. J. Chem. Model*, 4 (1), 13-20, (2012).
- [3] Kong, F.A. The periodicity of diatomic molecules. *J. Mol. Struct.* 90, 17-28 (1982).
- [4] Kong, F. A., Wu WeiQian, Periodic tables of diatomic and triatomic molecules, *Sci. China Chem.* 55, 618-625 (2012), doi: 10.1007/s11426-012-4495-z.
- [5] Hefferlin, R. , J. Sackett, J. Tatum, Why do molecules echo atomic periodicity, *Int. J. Quant. Chem.* 2013. doi: 10.1002/qua.24469.
- [6] Kong, F. A., in Hefferlin, R. *Periodic Systems of Molecules and their Relation to the Systematic Analysis of Molecular Data*; Edwin Mellin Press: Lewiston, New York, 1989, chapter 11..
- [7] Hefferlin, R., Kronecker-product periodic systems of small gas-phase molecules and the search for order in atomic ensembles of any phase, *Comb. Chem. High Through. Screen.* 11, 690-706 (2008).
- [8] <http://webbook.nist.gov/chemistry/>
- [9] Kong, F. A. The periodicity of molecules, Mathematical Chemistry Workshop of the Americas, 2010, Bogota, Colombia, July 21-24, 2010.
- [10] Scerri, E. Some aspects of the metaphysics of chemistry and the nature of the elements, *Int. J. Found. Chem.* 11 (2), 127-145, (2005).
- [11] Latysheva, V. A., Hefferlin R. Periodic systems of molecules as elements of shchukarev's "supermatrix", *i.e.*, the chemical element periodic system. *J. Chem Inf. Comput. Sci.* 44, 1202-1209 (2004), Fig. 1
- [12] Herzberg, G. Infrared and Raman Spectra, D. Van Nostrand, New York, 1962.

- [13] Krasnov, K.S., *Molekulyarnye postoyannye neorganicheskikh soedineni. Khimiya*, 1979 (An earlier edition was translated into English: Schmorak, J., Trans., *Handbook of Molecular Constants of Inorganic Compounds*. Israel Program for Scientific Translation, 1970).
- [14] Lide, David R., Ed. *Handbook of Chemistry and Physics*, CRC Press Boca Raton, Florida, 2003-2004.
- [15] Huber, K.P., Herzberg, G. *Constants of diatomic molecules*, Van Nostrand Reinhold Company: New York, 1979.
- [16] Cavinaugh, R., Marsa, R., Robertson, J. Hefferlin, R. Adjacent DIM isoelectronic molecules and chemical similarity among triatomics, *J. Mol. Struct.* 382, 137-145 (1996).
- [17] <http://physics.nist.gov/cgi-bin/MolSpec/triperiodic>
- [18] Turney, J.M., Simmonett, A.C., Parrish, R.M., Hohenstein, E.G., Evangelista, F., Fermann, J.T., Mintz, B.J., Burns, L.A., Wilke, J.J., Abrams, M.L., Russ, N.J., Leininger, M.L., Janssen, C. L., Seidl, E.T., Allen, W.D., Schaefer, H.F., King, R.A. Valeev, E.F., Sherrill, C.D., Crawford, T. D., *WIREs Comput. Mol. Sci.* 2, 556 (2012). (doi: 10.1002/wcms.93).